Periodica Polytechnica
Civil Engineering

61(2), pp. 282–291, 2017
https://doi.org/10.3311/PPci.8210

RESEARCH ARTICLE

Rapid Prediction of Moments in High-rise Composite Frames Considering Cracking and Time-effects

Umesh Pendharkar[1], K. A. Patel[2], Sandeep Chaudhary[3*], A. K. Nagpal[2]

Received 06 May 2015; Revised 14 April 2016; Accepted 29 June 2016

Abstract

There can be a significant amount of moment redistribution in steel concrete composite frames due to cracking, creep and shrinkage in concrete. In the present study, neural network models have been developed for rapid prediction of the inelastic moments (typically for 20 years considering cracking, creep and shrinkage in concrete) in high rise composite frames. The possibility of sagging moment being developed at ends of beams due to the substantial differential shortening of adjacent columns has also been taken into account. Closed form expressions, based on the weights and biases of the trained neural networks, are proposed to predict the inelastic moments from the elastic moments (neglecting cracking and time effects). The expressions are verified for example frames of different number of spans and storeys and errors are found to be small. The expressions require computational effort that is a fraction of that required for the available methods.

Keywords

Composite frames, Cracking, Creep, Moment, Neural networks, Shrinkage

[1] School of Engineering and Technology,
Vikram University, Ujjain 456010, India
[2] Civil Engineering Department
Indian Institute of Technology Delhi, New Delhi 110016, India
[3] Civil Engineering Department
Malaviya National Institute of Technology, Jaipur 302017, India
* Corresponding author, e-mail: schaudhary.ce@mnit.ac.in

1 Introduction

There has been an extensive use of steel-concrete construction in high-rise building frames. The monolithic action of concrete slab and steel beams leads to the composite beam action (Fig. 1). There may be cracking of concrete slab of composite beams near interior joints where moments are higher than cracking moments. The time effects of creep and shrinkage in the concrete may lead to further progressive cracking and aging moment redistribution. Creep and shrinkage result in increase in elastic moments at joints [1–3]. The increase in moments at joints is primarily due to shrinkage, the contribution of creep being much smaller [1–3]. However, cracking in concrete results in lesser increase in moments as the portion of the concrete undergoing creep and shrinkage reduces [4–6].

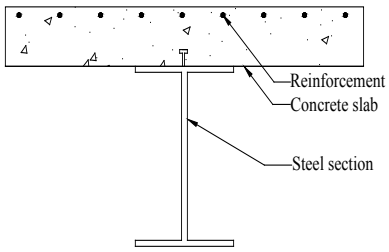

Fig. 1 Cross-section of composite beam

Methods are available in the literature for instantaneous and time-dependent analysis of the beams and frames, which take into account these moment redistributions. For instantaneous analysis, conventionally either an incremental or an iterative approach [1] is used which requires subdivisions and thereby numerical integration. The computational effort required in numerical integration may be considerable in case of large structures. For time-dependent analysis of composite structures, a large number of methods are available in the literature and they may be categorized in two types. Type 1 methods are numerical in nature and require large computational effort [6–9] and Type 2 methods are analytical in nature and are computationally efficient but these methods do not take into account all the aspects [4–5, 10]. A hybrid analytical-numerical procedure

has been developed by the authors to take into account the nonlinear effects of concrete cracking and time-dependent effects of creep and shrinkage in composite frames [3]. The procedure is efficient but the computational effort may again become considerable for large composite building frames. This effort may be many times more than that required for the elastic analysis (neglecting cracking and time effects in concrete). The use of neural network models may be made to drastically reduce the computational effort in such cases.

Soft computing techniques (neural networks, genetic algorithms etc.) have been extensively used in the field of structural engineering for prediction of the parameters without any rigorous analysis and experiments [11–15]. Many researchers have proposed the closed form expressions using the weight matrices and activated function of the trained neural network. Some of the closed form expressions obtained from the trained neural networks include determination of distortional buckling stress in cold-formed steel members [16], estimation of ultimate pure bending of fabricated and cold-formed steel circular tubes [17], prediction of base shear of steel frame structures [18], estimation of distortional buckling stress in elliptical hollow section tubes [19], evaluation of deflections in composite bridges considering flexibility of shear connectors, concrete cracking and shear lag effect [20] and prediction of effective moment of inertia in reinforced concrete beams [21]. Such closed form expressions are useful to predict the parameters in every day design with acceptable accuracy. These studies reveal the strength of neural networks in predicting the solutions of different structural engineering problems.

Neural networks have been used to predict the design quantities in steel-concrete composite structures also including bending moments and deflections in continuous composite beams considering concrete cracking [22–23], deflections in continuous composite beams and frames considering cracking and time effects in concrete [24–25]. Pendharkar et al. [26] have developed the neural networks for prediction of bending moments in composite frames considering cracking and time effects in concrete. However, these neural networks do not take into account the sagging moments developed in beams due to the substantial differential shortening of adjacent columns of high rise frames. The neural networks are therefore valid for low to moderately high frames and have limited applicability.

In this paper, a methodology has been presented for rapid prediction of inelastic moments in high-rise composite frames. The closed form expressions, obtained from the trained neural networks, are proposed to predict the inelastic moments, M^i (typically for 20 years, considering cracking and time effects in concrete) from elastic moments, M^e (neglecting cracking and time effects in concrete). M^e can be obtained from any of the readily available software and requires little computational effort. The training, validating, and testing data sets are generated using an analytical-numerical hybrid procedure of analysis [3]. The expressions also take into account the sagging moments developed in beams due to the substantial differential shortening of adjacent columns in high-rise frames. The proposed expressions are verified for example frames of different number of spans and storeys and errors are shown to be small. The expressions can be used in every day design as they enable a rapid prediction of inelastic deflections with reasonable accuracy for practical purposes without detailed complex analysis and require computational effort that is a fraction of that required for the available methods in the literature.

2 Analysis of composite frames

For generalized and efficient neural networks, a huge number of training data sets are required; for the generation of which, a highly efficient method is desirable. A hybrid analytical-numerical procedure has therefore been adopted which takes into account the nonlinear effects of concrete cracking near interior joints and time-dependent effects of creep and shrinkage in composite frames [3]. The procedure is analytical at the elemental level and numerical at the structural level. A cracked span length beam element, consisting of two cracked zones of length x_A and x_B at the ends A and B respectively and an uncracked zone in the middle (Fig. 2), has been used in the procedure [3]. For a completely cracked span length beam element of total length L, x_A and x_B would be equal to $L/2$ and for a completely uncracked beam element x_A and x_B would be equal to zero. Slip at the interface of the concrete slab and the steel section is neglected assuming that shear connectors are at a sufficiently close spacing. The effect of slip has been reported to be small in comparison to the time-dependent deformations [27].

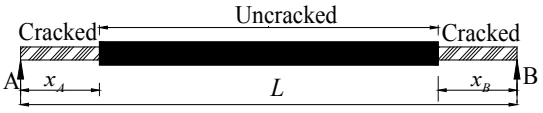

Fig. 2 Cracked span length beam element

The analysis in the hybrid procedure is carried out in two parts. In the first part, an instantaneous analysis is carried out using an iterative method. In the second part, a time-dependent analysis is carried out by dividing the time into a number of time intervals to take into account the progressive nature of cracking of concrete (Fig. 3). As shown in figure, crack lengths are assumed to be constant in a time-interval and revised at the end of each time interval. The aged-adjusted effective modulus method, AEMM [28] is used for predicting the creep and shrinkage effects which has been used earlier also for composite frames [29]. CEB-FIP 90 [30] is used for predicting the short term as well as time-dependent properties of the concrete.

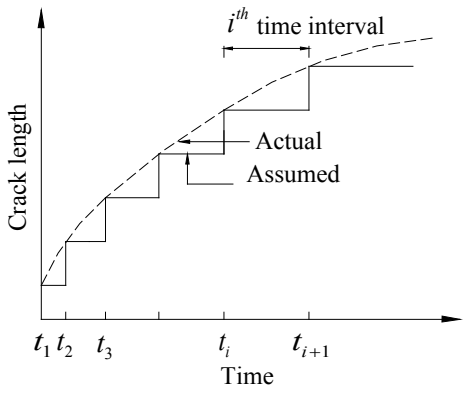

Fig. 3 Progressive nature of cracking

The procedure has been validated by comparison with the experimental, analytical, and finite element method results [3].

3 Probable structural parameters

As stated earlier in section 1, instantaneous cracking in composite beams of high-rise frames occurs in the end portions (where hogging moments occur) when tensile stresses are higher than the tensile strength of concrete. This instantaneous cracking may further progress due to time effects. The elastic bending moment, M^e at an instantaneous stage gets redistributed due to cracking and there is a further redistribution owing to time effects of creep and shrinkage leading to M^i at a final stage (typically 20 years).

Consider an intermediate floor of a frame with the loading (Fig. 4a). The nature of elastic moment diagram and inelastic moment diagram at a joint, j of an intermediate floor of a frame is shown in the Fig. 4b.

Since cracking and creep and shrinkage effects, in the type of frames being considered, are confined to beams only, it may be postulated based on the studies on the composite frames [26], that in order to establish redistribution of moment at a joint j with sufficient accuracy, cracking at the joint and adjacent joints (joint j and joint $j + 1$) only needs to be considered. Keeping this in view, the following input parameters for an internal joint j of a frame are identified as:

1. Cracking moment ratio on the right side of joint $j - 1$, $R^r_{j-1}\left(= M^{e,r}_{j-1} / M^{cr}\right)$,
2. Cracking moment ratio on the left side of joint j, $R^l_j \left(= M^{e,l}_j / M^{cr}\right)$,
3. Cracking moment ratio on the right side of joint j, $R^r_j \left(= M^{e,r}_j / M^{cr}\right)$,
4. Cracking moment ratio on the left side of joint $j + 1$, $R^l_{j+1}\left(= M^{e,l}_{j+1} / M^{cr}\right)$,
5. Stiffness ratio of adjacent spans at joint j, S_{j-1}/S_j ($S_j = EI^{un} / l_j$, where E = modulus of elasticity of concrete, and I^{un} = transformed moment inertia of composite section about top fiber, the reference axis),
6. Load ratio of the adjacent spans at joint j, w_{j-1}/w_j, ,
7. Composite inertia ratio, I^{cr} / I^{un} (I^{cr} = transformed moment of inertia of steel section and reinforcement about top fiber, the reference axis),
8. Age of loading, t_0,
9. Grade of concrete, Gr.

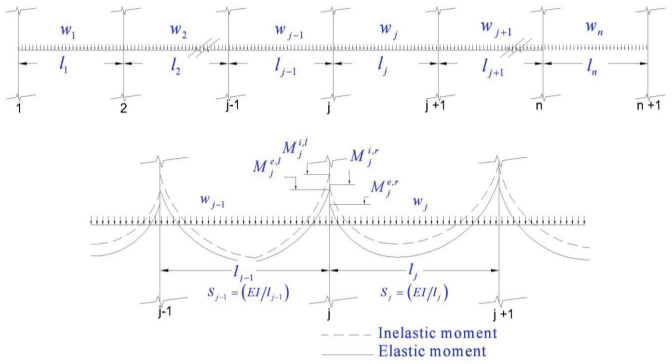

Fig. 4 (a) An intermediate floor of a frame with the loading, and (b) natures of elastic and inelastic bending moments

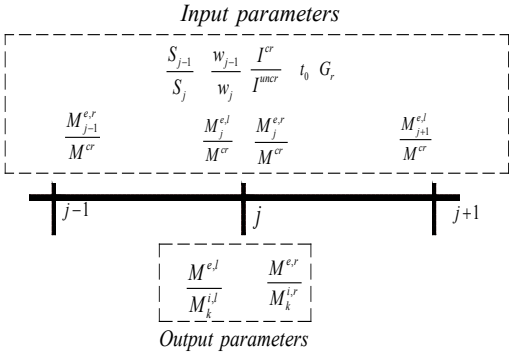

Fig. 5 Schematic representation of input and output parameters

These nine input parameters are schematically shown in Fig. 5. The two outputs for the neural network model for an internal joint, j, are considered as $M^{e,l}_j / M^{i,l}_j$ (inelastic moment ratio to the left of joint j) and $M^{e,r}_j / M^{i,r}_j$ (inelastic moment ratio to the right of joint j).

The practical ranges for the different structural parameters are considered as: R^r_{j-1}, R^l_j, R^r_j, R^l_{j+1} = -4.0 to 4.0; S_{j-1}/S_j = 0.25 to 4.0; w_{j-1}/w_j = 0.25 to 4.0; I^{cr} / I^{un} = 0.38 to 0.54; t_0 = 7 days to 21 days; Gr = 20 N/mm^2 to 40 N/mm^2. In order to incorporate sagging moments developed in beams due to the substantial differential shortening of adjacent columns which are likely to be observed in high rise frames, the negative values of the structural parameters R^r_{j-1}, R^l_j, R^r_j, R^l_{j+1} are considered.

It may be noted that the ratio of beam stiffness to column stiffness is not taken as an input parameter; since in the output parameters $M^{e,l}_j / M^{i,l}_j$ and $M^{e,r}_j / M^{i,r}_j$, both M^e and M^i may be assumed to be affected approximately to the same degree by variation in ratio of beam to column stiffness.

All the neural networks are trained for a particular value of relative humidity, *RH* (= 85%). The output parameter for other values of relative humidity can be estimated in a manner similar to that explained by Pendharkar et al. [26].

4 Architecture of neural network models

The neural networks chosen in the present study are multilayered feed-forward networks with neurons in all the layers fully connected in feed forward manner (Fig. 6). Various algorithms and activation functions are available in the above discussed literature. However, the back propagation algorithm has been used successfully for many science and engineering applications and is considered as one of the efficient, popular and successful algorithm in engineering applications [31-32]. Therefore, the back propagation algorithm along with sigmoid activation function is used for this study. The back propagation algorithm updates the weight and bias values to achieve a desired input-output relationship in each of the iteration that generates output values which are closer to the target values. MATLAB Neural Network tool [33] has been used for training, validating and testing of the neural networks. One hidden layer is chosen and the number of neurons in the layer is decided in the learning process by trial and error.

First, consider the neural network model for an internal joint. As stated earlier in section 2, the neural network model consists of nine input parameters and two output parameters. The nine input parameters are: R^r_{j-1}, R^l_j, R^r_j, R^l_{j+1}, S_{j-1} / S_j, w_{j-1} / w_j, I^{cr} / I^{un}, t_0 and Gr and the two output parameters are: $M^{e,l}_j \big/ M^{i,l}_j$ and $M^{e,r}_j \big/ M^{i,r}_j$.

Next, consider the neural network model for an external joint. The input parameters R^r_{j-1}, $S_{j-1} \big/ S_j$ and w_{j-1} / w_j are absent for left external joint (j = 1), whereas, the input parameters R^l_{j+1}, S_{j-1} / S_j and w_{j-1} / w_j are absent for right external joint. The input parameters for left external joint (joint 1) are: R^r_1, R^l_2, I^{cr} / I^{un}, t_0 and Gr , whereas, the parameters for right external joint (joint n + 1) are: R^r_n, R^l_{n+1}, I^{cr} / I^{un}, t_0 and Gr . The output parameters are $M^{e,r}_1 \big/ M^{i,r}_1$ and $M^{e,l}_{n+1} \big/ M^{i,l}_{n+1}$ for left external joint and right external joint respectively.

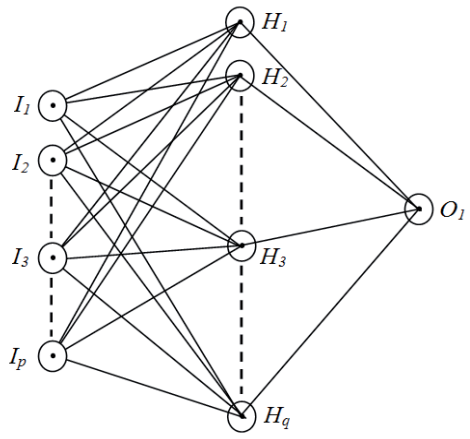

Fig. 6 A typical neural network model

The training data sets are generated for 37th, 38th, 39th, 40th floors of a forty storey-seven bay frame, henceforth designated as data generation frame. It is postulated that neural network models based on these training data sets are applicable for predicting $M^{e,l}_j / M^{i,l}_j$ and $M^{e,r}_j / M^{i,r}_j$ for frames of any number of spans and storeys.

Two neural network models, one each for external joints and internal joints and designated as Net-E, and Net-I, respectively, are trained. Input data sets are chosen to cover the entire practical range of parameters and sufficiently large number of values of each of the parameters. The training, validating, and testing data sets, typically for interior joint, consist of nine input parameters and two output parameters. In order to have specified values of nine input parameters of a data set, an iterative procedure needs to be followed. The variables, for the data generation frame, are seven span lengths, seven corresponding loadings on the spans, cross-sectional properties, grade of concrete and age of loading in the hybrid analytical-numerical iterative procedure [3]. The values of the variables are adjusted in such a manner that the specified values of nine input parameters are achieved. Similar exercise is done for exterior spans with six input parameters.

Total 8,640 and 18,600 data sets, in the practical range of the parameters, are generated for Net-E, and Net-I respectively. To bring all non fictitious input parameters and output parameters in the range -1.0 to 1.0, the input as well as the output parameters are divided by the normalization factors given in Table 1.

Table 1 Normalization factors

Parameters		Network	
		Net-E	Net-I
Input	R^r_{j-1}	4	4
	R^l_j	4	4
	R^r_j	4	4
	R^l_{j+1}	4	4
	S_{j-1} / S_j	-	4
	w_{j-1} / w_j	-	4
	I^{cr} / I^{un}	1	1
	t_0 (days)	21	21
	Gr (N/mm^2)	40	40
Output	$M^{e,l}_j / M^{i,l}_j$	-	7 (Bias = 2)
	$M^{e,r}_j / M^{i,r}_j$	1.3	7 (Bias = 2)

As stated earlier, the training is carried out using the MATLAB Neural Network tool [33]. For each network, 70% of the data sets are used for the training (as training patterns) whereas 15% of the data sets are used for the validating and testing each. For this partitioning, 'hold out method' [34], in which partitioning is done randomly, has been adopted. For training, several trials are carried out with different numbers of neurons in the hidden layer. Care is taken that the mean square error for test results does not increase with the number of neurons in hidden layer or epochs (overtraining). The architectures of the two optimum networks (number of input parameters-number of neurons in hidden layer-number of output parameters) along with the statistical parameters i.e. mean square error (MSE), mean absolute percentage error (MAPE), average absolute deviation (AAD), square of coefficient of correlation (R^2) and coefficient of variation (COV) of training, validating and testing data sets are given in Table 2. All parameters indicate a good performance.

Table 2 Statistical parameters on neural networks

Sets	Parameters	Network (Architecture)	
		Net-E (5-9-1)	Net-I (9-14-2)
Training	MSE	0.00151	0.00192
	MAPE	4.10259	5.56894
	AAD	4.07064	6.36540
	R^2	0.95750	0.94958
	COV	5.29704	6.92775
Validating	MSE	0.00160	0.00197
	MAPE	4.11565	5.84112
	AAD	4.08460	6.49102
	R^2	0.94455	0.94114
	COV	5.42761	7.05987
Testing	MSE	0.00182	0.00205
	MAPE	4.22319	5.00265
	AAD	4.17958	6.88144
	R^2	0.92363	0.93008
	COV	5.78874	7.12134

5 Closed form expressions

For the ease of practicing engineers and users, it is desirable to propose simplified closed form expressions for the prediction of moments. The trained neural networks may be used to develop the required closed form expressions. Since the sigmoid function has been used as the activation function, the outputs O_1 ($=M_j^{e,l}/M_j^{i,l}$) and O_2 ($=M_j^{e,r}/M_j^{i,r}$) are given as below [20–21]

$$O_1 = \frac{1}{1+e^{-\left(bias_{01}+\sum_{k=1}^{r}\frac{w_{k,1}^{ho}}{1+e^{-Hk}}\right)}} \tag{1}$$

$$O_2 = \frac{1}{1+e^{-\left(bias_{02}+\sum_{k=1}^{r}\frac{w_{k,2}^{ho}}{1+e^{-Hk}}\right)}} \tag{2}$$

$$H_k = \sum_{j=1}^{q} w_{j,k}^{ih} \times I_j + bias_k \tag{3}$$

where, q is the number of input parameters; r is the number of hidden neurons; $bias_k$ is the bias of k^{th} hidden neuron (h_k); $bias_{o1}$; $bias_{o2}$ are the bias of output neurons; $w_{j,k}^{ih}$ is the weight of the link between I_j and h_k; $w_{k,1}^{ho}$ is the weight of the link between h_k and O_1; $w_{k,2}^{ho}$ is the weight of the link between h_k and O_2.

The inelastic moments at left and right side of joints are then given as

$$M_j^{i,l} = M_j^{e,l}/O_1; \quad M_j^{i,r} = M_j^{e,r}/O_2 \tag{4}$$

The value of O_1 and O_2 may be obtained as given in Appendix A.

6 Verification of neural networks models

Trained neural networks are verified for two example frames of 50 storey-5 bay (EF1) and 20 storey-10 bay (EF2) with a wide variation of input parameters (Fig. 7). Example frames have been chosen in such a way that none of the combinations of input parameters has been used in the training, validating and testing. Span lengths and load intensities of the frames are given in Fig. 7 and Table 3. The floor height and age of loading are taken as 3.0 m and 10 days respectively for both the frames. In both the frames, 1000 mm wide and 70 mm thick concrete slab with M32 grade of concrete and a steel I section with a cross-sectional area of 5.14×10^{-3} m^2, moment of inertia of 8.50×10^{-5} m^4 about its major principle axis and depth of 305 mm, form the composite beams at all the floors. The slabs of composite beams of the frame have a reinforcement of area 113 mm^2 placed at a distance of 15 mm from the top fibre. The columns of the frame EF1 consist of rolled steel sections 914 × 305 UB 253 for storey 1–20, 610 × 305 UB 238 for storey 21–40 and 406 × 178 UB 74 for storey 41–50 whereas the columns of the frame EF2 consist of 203 × 133 UB 25 at all the floors. The beam to column stiffness varies along the height of the frame in frame EF1 wheras it is constant in frame EF2.

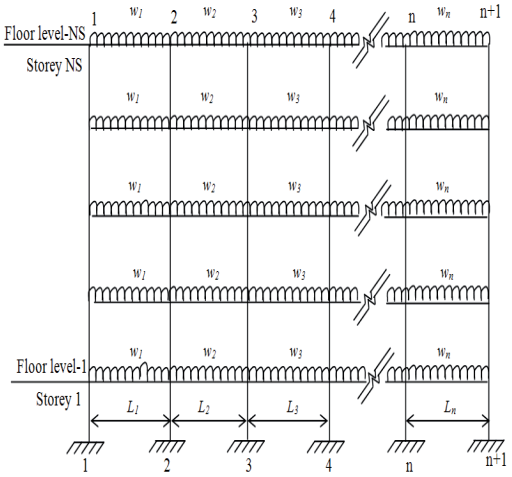

Fig. 7 Schematic representation of example frames

Table 3 Details of example frames

Frame	Spans	Property	
		Length (m)	Load (kN/m)
EF1	1	5.0	5.0
	2	6.0	8.0
	3	8.0	6.0
	4	6.0	8.0
	5	5.0	5.0
EF2	1	5.7	24.5
	2	8.9	28.2
	3	6.4	25.2
	4	5.4	28.2
	5	7.9	29.2
	6	5.4	28.1
	7	7.9	25.9
	8	4.4	43.1
	9	8.4	23.8
	10	6.9	23.9

Results are compared for typical floor levels 10, 30 and 40 of the frame EF1 and for typical floor level 15 of the frame EF2. The network Net-E is used for external joints, whereas network Net-I is used for internal joints. Table 4 shows the values of the normalised input parameters for the external and internal joints of the frame EF1 and EF2. As stated earlier, these parameters are in different permutations than those used in training, validating, and testing.

Table 5 shows the values of elastic moments, $M_j^{e,l}$ and $M_j^{e,r}$, and inelastic moments, $M_j^{i,l}$ and $M_j^{i,r}$ obtained from the hybrid procedure and the neural networks for both frames. For the frame EF1, the maximum absolute error in the prediction of inelastic moments is 4.73% for exterior joints and 10.83% for interior joints which is acceptable for practical design. Similarly, for the frame EF2, the maximum absolute error in the prediction of inelastic moments is 8.06% for exterior joints and 10.23% for interior joints which is also acceptable for practical design. This shows the efficacy of developed neural network models for high-rise frames with any number of spans and storeys.

7 Conclusions

In this paper, the closed form expressions have been presented for rapid prediction of the inelastic moments in high-rise steel-concrete composite frames, from the elastic moments. Two neural network models, Net-E and Net-I, applicable for exterior joints and interior joints respectively, have been developed to obtain the close form expressions. These expressions take into account cracking and time-effects (i.e. creep and shrinkage) in concrete as well as the sagging moments developed in beams due to the substantial differential shortening of adjacent columns in high-rise frames. The expressions have been verified with example high-rise frames. The overall root mean square percentage error for both example frames, considered for validation is 5.66% for all exterior and interior joints, which is acceptable for practical design. The proposed expressions can predict the inelastic moments, in high-rise composite frames, with reasonable accuracy from the elastic moments, which in turn, can be obtained from any of the readily available software. The computational effort required is a fraction of that required for the available methods. The closed form expressions are applicable for high-rise composite frames of any number of spans and storeys.

The methodology of the present study can be developed further for rapid prediction of inelastic deflections in high-rise composite frames also where the effect of axial shortening of the columns is significant.

Notations

E	modulus of elasticity of concrete
Gr	grade of concrete
H	hidden neuron
I	Input parameter
I^{un}	transformed moment of inertia of composite section
I^{cr}	transformed moment of inertia of steel section and reinforcement
M	bending moment
O_1, O_2	output parameters
$R^l_{j+2}, R^l_j, R^l_{j+1}, R^r_{j-1}, R^r_j, R^r_{j+1}$	cracking moment ratios
RH	relative humidity
S	stiffness
l	span length
n	number of spans/bays
t_0	age of loading
w	uniformly distributed load

Subscript

j	support or span number
p	number of input parameters/neurons
q	number of hidden neurons

Superscript

cr	cracking
e	elastic
i	inelastic
l	left side of a joint
r	right side of a joint

Table 4 Details of example frames

Frame	Network used	Floor level	Joint No.	R^r_{j-1}	R^l_j	R^r_j	R^l_{j+1}	S_{j-1} / S_j	w_{j-1} / w_j	I^{cr} / I^{un}	t_0 (days)	Gr (N/mm^2)
EF1	Net-E	40th	1	-	-	0.4700	-0.2076	-	-	0.4332	0.4762	0.8000
			6	-0.2076	0.4700	-	-	-	-	0.4332	0.4762	0.8000
		30th	1	-	-	0.4377	-0.1862	-	-	0.4332	0.4762	0.8000
			6	-0.1862	0.4377	-	-	-	-	0.4332	0.4762	0.8000
		10th	1	-	-	0.2595	-0.0641	-	-	0.4332	0.4762	0.8000
			6	-0.0641	0.2595	-	-	-	-	0.4332	0.4762	0.8000
	Net-I	40th	2	0.4700	-0.2076	0.3853	-0.2213	0.3000	0.1563	0.4332	0.4762	0.8000
			3	0.3853	-0.2213	0.0836	0.0836	0.3333	0.3333	0.4332	0.4762	0.8000
			4	0.0836	0.0836	-0.2213	0.3853	0.1875	0.1875	0.4332	0.4762	0.8000
			5	-0.2213	0.3853	-0.2076	0.4700	0.2083	0.4000	0.4332	0.4762	0.8000
		30th	2	0.4377	-0.1862	0.3619	-0.1841	0.3000	0.1563	0.4332	0.4762	0.8000
			3	0.3619	-0.1841	0.0962	0.0962	0.3333	0.3333	0.4332	0.4762	0.8000
			4	0.0962	0.0962	-0.1841	0.3619	0.1875	0.1875	0.4332	0.4762	0.8000
			5	-0.1841	0.3619	-0.1862	0.4377	0.2083	0.4000	0.4332	0.4762	0.8000
		10th	2	0.2595	-0.0641	0.2398	0.0148	0.3000	0.1563	0.4332	0.4762	0.8000
			3	0.2398	0.0148	0.1639	0.1639	0.3333	0.3333	0.4332	0.4762	0.8000
			4	0.1639	0.1639	0.0148	0.2398	0.1875	0.1875	0.4332	0.4762	0.8000
			5	0.0148	0.2398	-0.0641	0.2595	0.2083	0.4000	0.4332	0.4762	0.8000
EF2	Net-E	15th	1	-	-	0.3397	0.3099	-	-	0.4332	0.4762	0.8000
			11	0.5880	0.5292	-	-	-	-	0.4332	0.4762	0.8000
	Net-I	15th	2	0.3397	0.3099	0.9846	0.9519	0.3904	0.2172	0.4332	0.4762	0.8000
			3	0.9846	0.9519	0.4419	0.4103	0.1798	0.2798	0.4332	0.4762	0.8000
			4	0.4419	0.4103	0.3515	0.3042	0.2109	0.2234	0.4332	0.4762	0.8000
			5	0.3515	0.3042	0.7999	0.7621	0.3657	0.2414	0.4332	0.4762	0.8000
			6	0.7999	0.7621	0.3485	0.3004	0.1709	0.2598	0.4332	0.4762	0.8000
			7	0.3485	0.3004	0.7018	0.6655	0.3657	0.2712	0.4332	0.4762	0.8000
			8	0.7018	0.6655	0.3522	0.2637	0.1392	0.1502	0.4332	0.4762	0.8000
			9	0.3522	0.2637	0.7489	0.7117	0.4773	0.4527	0.4332	0.4762	0.8000
			10	0.7489	0.7117	0.5879	0.5292	0.2054	0.2297	0.4332	0.4762	0.8000

Table 5 Comparison of inelastic moments for example frames

Frame	Floor level	Joint No. j	Elastic moment (kNm)		Inelastic moment (kNm)			
					Neural network		Hybrid procedure	
			$M_j^{e,l}$	$M_j^{e,r}$	$M_j^{e,l}$	$M_j^{e,r}$	$M_j^{e,l}$	$M_j^{e,r}$
EF1	40th	1	-	61.58	-	68.65	-	65.78
		2	-27.21	50.49	-16.31	70.17	-17.53	65.31
		3	-29.00	10.95	-13.15	31.05	-12.89	30.26
		4	10.95	-29.00	28.52	-13.87	30.26	-12.89
		5	50.49	-27.21	70.65	-16.33	65.31	-17.53
		6	61.58	-	68.65	-	65.78	-
	30th	1	-	57.36	-	65.13		62.19
		2	-24.39	47.42	-12.63	66.81	-13.52	63.66
		3	-24.13	12.61	-9.88	31.77	-9.24	31.76
		4	12.61	-24.13	28.32	-9.63	31.76	-9.24
		5	47.42	-24.39	67.41	-12.54	63.66	-13.52
		6	57.36	-	65.13	-	62.19	-
	10th	1	-	34.00	-	43.27	-	43.64
		2	-8.40	31.42	10.81	42.48	9.93	47.00
		3	1.94	21.47	17.02	38.07	16.25	39.19
		4	21.47	1.94	40.21	15.28	39.19	16.25
		5	31.42	-8.40	43.09	9.14	47.00	9.93
		6	34.00	-	43.27	-	43.64	-
EF2	15th	1	-	64.26	-	69.56	-	71.02
		2	58.62	186.25	71.41	200.23	69.78	181.65
		3	180.06	83.58	184.15	90.26	178.82	89.94
		4	77.61	66.49	88.36	75.33	84.75	74.72
		5	57.54	151.32	70.44	162.92	71.39	150.54
		6	144.17	65.92	148.82	73.69	146.43	74.50
		7	56.82	132.76	69.33	143.15	69.95	133.06
		8	125.88	66.63	131.18	74.08	129.10	76.23
		9	49.88	141.66	60.97	152.63	67.07	142.71
		10	134.62	111.22	138.87	118.14	137.58	120.56
		11	100.10	-	121.11	-	112.08	-

References

[1] Ghali, A., Favre, R., Elbadry, M. "Concrete Structures: Stresses and Deformations." Spon Press, UK, 2002.

[2] Pendharkar, U., Chaudhary, S., Nagpal, A. K. "Neural networks for bending moments in continuous composite beams considering cracking and time effects in concrete." *Engineering Structures*. 29(9), pp. 2069-2079. 2007. DOI: 10.1016/j.engstruct.2006.11.009

[3] Chaudhary, S., Pendharkar, U., Nagpal, A. K. "Hybrid procedure for cracking and time-dependent effects in composite frames at service load." *Journal of Structural Engineering*. 133(2), pp. 166-175. 2007. DOI: 10.1061/(ASCE)0733-9445(2007)133:2(166)

[4] Gilbert, R. I., Bradford, M. A. "Time-dependent behavior of composite beams at service loads." *Journal of Structural Engineering*. 121(2), pp. 319-327. 1995. DOI: 10.1061/(ASCE)0733-9445(1995)121:2(319)

[5] Bradford, M. A., Manh, H. V., Gilbert, R. I. "Numerical analysis of continuous composite beams at service loading." *Advances in Structural Engineering*. 5(1), pp. 1-12. 2002. DOI: 10.1260/1369433021502498

[6] Kwak, H. G., Seom,Y. J. "Long term behavior of composite girder bridges." *Computers and Structures*. 74(5), pp. 583-599. 2000. DOI: 10.1016/S0045-7949(99)00064-4

[7] Cruz, P. J. S., Mari, A. R., Roca, P. "Non-linear time dependent analysis of segmentally constructed structures." *Journal of Structural Engineering*. 124(3), pp. 278-287. 1998. DOI: 10.1061/(ASCE)0733-9445(1998)124:3(278)

[8] Mari, A. "Numerical simulation of the segmental construction of three dimensional concrete frames." *Engineering Structures*. 22(6), pp. 585-596. 2000. DOI: 10.1016/S0141-0296(99)00009-7

[9] Fragiacomo, M., Amadio, C., Macorini, L. "Finite element model for collapse and long-term analysis of steel-concrete composite beams." *Journal of Structural Engineering*. 130(3), pp. 489-497. 2004. DOI: 10.1061/(ASCE)0733-9445(2004)130:3(489)

[10] Amadio, C., Fragiacomo, M. "A simplified approach to evaluate creep and shrinkage effects in steel concrete composite beams." *Journal of Structural Engineering*. 123(9), pp. 1153-1162. 1997. DOI: 10.1061/(ASCE)0733-9445(1997)123:9(1153)

[11] Kim, D. K., Kim, D. H., Cui, J., Seo, H. Y., Lee, Y. H. "Iterative neural network strategy for static model identification of an FRP deck." *Steel and Composite Structures*. 9(5), pp. 445-455. 2009. DOI: 10.12989/scs.2009.9.5.445

[12] Gupta, T., Sharma, R. K. "Structural analysis and design of buildings using neural networks: a review." *International Journal of Engineering and Management Sciences*, 2(4), pp. 216-220. 2011.

[13] Mohammadhassani, M., Nezamabadi-Pour, H., Jumaat, M. Z., Jameel, M., Arumugam, A. M. S. "Application of artificial neural networks (ANNs) and linear regressions (LR) to predict the deflection of concrete deep beams." *Computers and Concrete*. 11(3), pp. 237-252. 2013. DOI: 10.12989/cac.2013.11.3.237

[14] Mohammadhassani, M., Nezamabadi-Pour, H., Jumaat, M. Z., Jameel, M., Hakim, S. J. S., Zargar, M. "Application of the ANFIS model in deflection prediction of concrete deep beam." *Structural Engineering and Mechanics*. 45(3), pp. 319-332. 2013. DOI: 10.12989/sem.2013.45.3.323

[15] Srisanthi, V. G., Keshav, L., Poorna Kumar, P., Jayakumar, T. "Finite element and experimental analysis of 3D masonry compressed stabilised earth block and brick building models against earthquake forces." *Periodica Polytechnica Civil Engineering*. 58(3), pp. 255-265. 2014. DOI: 10.3311/PPci.7443

[16] Pala, M. "A new formulation for distortional buckling stress in cold-formed steel members." *Journal of Constructional Steel Research*. 62(7), pp. 716-722. 2006. DOI: 10.1016/j.jcsr.2005.09.011

[17] Shahin, M., Elchalakani, M. "Neural networks for modelling ultimate pure bending of steel circular tubes." *Journal of Constructional Steel Research*. 64(6), pp. 624-633. 2008. DOI: 10.1016/j.jcsr.2007.12.001

[18] Caglar, N., Pala, M., Elmas, M., Eryılmaz, D. M. "A new approach to determine the base shear of steel frame structures." *Journal of Constructional Steel Research*. 65(1), pp. 188-195. 2009. DOI: 10.1016/j.jcsr.2008.07.012

[19] Dias, J. L. R., Silvestre, N. "A neural network based closed-form solution for the distortional buckling of elliptical tubes." *Engineering Structures*. 33(6), pp. 2015-2024. 2011. DOI: 10.1016/j.engstruct.2011.02.038

[20] Tadesse, Z., Patel, K. A., Chaudhary, S., Nagpal, A. K. "Neural networks for prediction of deflection in composite bridges." *Journal of Constructional Steel Research*, 68(1), pp. 138-149. 2012. DOI: 10.1016/j.jcsr.2011.08.003

[21] Patel, K. A., Bhardwaj, A., Chaudhary, S., Nagpal, A. K. "Explicit expression for effective moment of inertia of RC Beams." *Latin American Journal of Solids and Structures*. 12(2), pp. 542-560. 2015.

[22] Chaudhary, S., Pendharkar, U., Nagpal, A. K. "Bending moment prediction for continuous composite beams by neural networks." *Advances in Structural Engineering*. 10(4), pp. 439-454. 2007. DOI: 10.1260/136943307783239390

[23] Chaudhary, S., Pendharkar, U., Patel, K. A., Nagpal, A. K. "Neural networks for deflections in continuous composite beams considering concrete cracking." *Iranian Journal of Science and Technology Transactions of Civil Engineering*. 38(C1+), pp. 205-221. 2014.

[24] Pendharkar, U., Chaudhary, S., Nagpal, A. K. "Neural networks for inelastic mid-span deflections in continuous composite beams." *Structural Engineering and Mechanics*. 36(2), pp. 165-179. 2010. DOI: 10.12989/sem.2010.36.2.165

[25] Pendharkar, U., Patel, K. A., Chaudhary, S., Nagpal, A. K. "Rapid prediction of long-term deflections in composite frames." *Steel and Composite Structures*. 18(3), pp. 547-563. 2015. DOI: 10.12989/scs.2015.18.3.547

[26] Pendharkar, U., Chaudhary, S., Nagpal, A. K. "Prediction of moments in composite frames considering cracking and time effects using neural network models." *Structural Engineering and Mechanics*. 39(2), pp. 267-285. 2011. DOI: 10.12989/sem.2011.39.2.267

[27] Wang, W. W., Dai, J. G., Guo, L., Huang, C. K. "Long-term behavior of prestressed old-new concrete composites beams." *Journal of Bridge Engineering*. 16(2), pp. 275-285. 2011. DOI: 10.1061/(ASCE)BE.1943-5592.0000152

[28] Bazant, Z. P. "Prediction of concrete creep-effects using age adjusted effective modulus method." *ACI Journal*. 69(4), pp. 212-217. 1972. DOI: 10.14359/11265

[29] Chowdhary, P., Sharma, R. K. "Evaluation of creep and shrinkage effects in composite tall buildings." *The Structural Design of Tall and Special Buildings*. 20(7), pp. 871-880. 2011. DOI: 10.1002/tal.584

[30] CEB-FIP "*Model code for concrete structures*." Thomas Telford, UK, 1993.

[31] Tarawneh, B., Nazzal, M. D. "Optimization of resilient modulus prediction from FWD results using artificial neural network." *Periodica Polytechnica Civil Engineering*. 58(2), pp. 143-154. 2014. DOI: 10.3311/PPci.2201

[32] Üneş, F., Demirci, M., Kişi, Ö. "Prediction of millers ferry dam reservoir level in USA using artificial neural network." *Periodica Polytechnica Civil Engineering*. 59(3), pp. 309-318. 2015. DOI: 10.3311/PPci.7379

[33] "*MATLAB 7.8 Neural networks toolbox user's guide*." USA, 2009.

[34] Reich, Y., Barai, S. V. "Evaluating machine learning models for engineering problems." *Artificial Intelligence in Engineering*. 13(3), pp. 257-272. 1999. DOI: 10.1016/S0954-1810(98)00021-1

Appendix A

Closed form expressions for O_1 and O_2

A.1. Right exterior joints

$$O_1 = \left[\frac{1.30}{1 + e^{-\left(-5.92 + \frac{1.35}{1+e^{-H_1}} + \frac{5.84}{1+e^{-H_2}} + \frac{5.05}{1+e^{-H_3}} + \frac{0.73}{1+e^{-H_4}} + \frac{15.16}{1+e^{-H_5}} + \frac{3.82}{1+e^{-H_6}} + \frac{0.27}{1+e^{-H_7}} + \frac{0.30}{1+e^{-H_8}} - \frac{0.31}{1+e^{-H_9}}\right)}} \right] \tag{A1}$$

A.2. Left exterior joints

$$\begin{bmatrix} H_1 \\ H_2 \\ H_3 \\ H_4 \\ H_5 \\ H_6 \\ H_7 \\ H_8 \\ H_9 \end{bmatrix} = \begin{bmatrix} 9.51 & 6.63 & -4.27 & 0.20 & -0.70 \\ 2.20 & 2.13 & -31.49 & -0.01 & -16.76 \\ -18.34 & 13.61 & 5.83 & 16.38 & -4.58 \\ -4.13 & -2.28 & -37.15 & 0.04 & -6.39 \\ 0.20 & -0.10 & 48.67 & 0.02 & -1.87 \\ -0.43 & 0.30 & 147.97 & -0.05 & -8.59 \\ 10.16 & -3.52 & -34.48 & 1.32 & 2.48 \\ 17.97 & -23.58 & 9.80 & 1.09 & 26.72 \\ -13.50 & -4.74 & 8.61 & -0.50 & 11.79 \end{bmatrix} \begin{bmatrix} R_j^r \\ R_{j+1}^l \\ I^{cr}/I^{un} \\ t_0 \\ Gr \end{bmatrix} + \begin{bmatrix} 0.16 \\ 35.11 \\ -19.00 \\ 24.79 \\ -16.35 \\ -52.97 \\ 5.07 \\ -23.87 \\ 6.33 \end{bmatrix} \tag{A2}$$

The value of O_1 for left exterior joints can be obtained by replacing R_j^r and R_{j+1}^l in Eq. (A2) with R_j^r and R_{j-1}^r respectively.

A.3. Interior joints

$$O_1 = \left[\frac{7.00}{1 + e^{-\left(0.68 + \frac{0.07}{1+e^{-H_1}} - \frac{0.04}{1+e^{-H_2}} - \frac{0.14}{1+e^{-H_3}} - \frac{13.68}{1+e^{-H_4}} - \frac{17.04}{1+e^{-H_5}} - \frac{0.10}{1+e^{-H_6}} + \frac{2.47}{1+e^{-H_7}} + \frac{29.65}{1+e^{-H_8}} - \frac{2.05}{1+e^{-H_9}} - \frac{0.60}{1+e^{-H_{10}}} - \frac{0.12}{1+e^{-H_{11}}} + \frac{0.01}{1+e^{-H_{12}}} - \frac{0.09}{1+e^{-H_{13}}} - \frac{0.13}{1+e^{-H_{14}}}\right)}} \right] - 2.00 \tag{A3}$$

$$O_2 = \left[\frac{7.00}{1 + e^{-\left(-17.35 + \frac{5.68}{1+e^{-H_1}} + \frac{0.41}{1+e^{-H_2}} - \frac{0.12}{1+e^{-H_3}} + \frac{0.20}{1+e^{-H_4}} + \frac{0.33}{1+e^{-H_5}} - \frac{1.06}{1+e^{-H_6}} - \frac{0.12}{1+e^{-H_7}} - \frac{0.51}{1+e^{-H_8}} + \frac{0.16}{1+e^{-H_9}} - \frac{0.07}{1+e^{-H_{10}}} + \frac{11.76}{1+e^{-H_{11}}} + \frac{17.99}{1+e^{-H_{12}}} - \frac{0.75}{1+e^{-H_{13}}} + \frac{0.94}{1+e^{-H_{14}}}\right)}} \right] - 2.00 \tag{A4}$$

$$\begin{bmatrix} H_1 \\ H_2 \\ H_3 \\ H_4 \\ H_5 \\ H_6 \\ H_7 \\ H_8 \\ H_9 \\ H_{10} \\ H_{11} \\ H_{12} \\ H_{13} \\ H_{14} \end{bmatrix} = \begin{bmatrix} 1.24 & 0.25 & 29.38 & -2.97 & 19.10 & -2.00 & -19.58 & -0.57 & -4.02 \\ 4.27 & -0.21 & 14.22 & -2.66 & 8.43 & -2.07 & -1.80 & -0.67 & -4.19 \\ -5.04 & 13.22 & 13.65 & -6.00 & 1.93 & -1.21 & -14.10 & -0.41 & 2.77 \\ 0.26 & 44.64 & -1.79 & 1.53 & -4.00 & 1.40 & -10.69 & -0.78 & -3.05 \\ -1.08 & 51.49 & 0.34 & 2.17 & -4.75 & 1.13 & -8.92 & -0.70 & -2.48 \\ 0.17 & -0.21 & -10.39 & 0.87 & 1.34 & 0.07 & -0.06 & -0.09 & -0.57 \\ -2.18 & 14.46 & 3.19 & 5.30 & -2.38 & 7.27 & 3.72 & -0.46 & -0.49 \\ -0.20 & 41.07 & -0.70 & 1.47 & -3.57 & 1.10 & -7.92 & -0.64 & -2.32 \\ -2.40 & 15.53 & 4.70 & 6.58 & 1.02 & 8.43 & 11.76 & -0.29 & 0.96 \\ 0.60 & -8.49 & 0.32 & 0.35 & -3.62 & 0.40 & -1.04 & -0.22 & -1.06 \\ 2.77 & 2.01 & 44.91 & -4.15 & 18.90 & -2.50 & -15.14 & -0.42 & -3.33 \\ -2.04 & -1.08 & -37.25 & 3.50 & -18.44 & 2.22 & 16.07 & 0.42 & 3.41 \\ 2.69 & -6.76 & 16.23 & 8.90 & 2.64 & 18.84 & -11.83 & -0.10 & 0.03 \\ -3.61 & -7.18 & -25.03 & 5.99 & 2.96 & 2.29 & -0.89 & -0.02 & 1.36 \end{bmatrix} \begin{bmatrix} R_{j-1}^r \\ R_j^l \\ R_j^r \\ R_{j+1}^r \\ S_{j-1}/S_j \\ w_{j-1}/w_j \\ I^{cr}/I^{un} \\ t_0 \\ Gr \end{bmatrix} + \begin{bmatrix} 12.90 \\ 8.78 \\ 5.52 \\ 11.49 \\ 12.21 \\ 0.17 \\ 1.02 \\ 9.75 \\ -5.56 \\ 2.84 \\ 9.12 \\ -10.10 \\ 5.15 \\ -5.03 \end{bmatrix} \tag{A5}$$